Kinetic degradation of guar gum in oilfield wastewater by photo-Fenton process

Shunwu Wang, Ziwang Li and Qinglong Yu

ABSTRACT

Guar gum is considered as a main component of oilfield wastewater. This work is intended to optimize the experimental conditions (H_2O_2 dosage, Fe^{2+} dosage, initial concentration of organics, initial pH and temperature) for the maximum oxidative degradation of guar gum by Fenton's reagent. The kinetics of guar gum removal were evaluated by means of the chemical oxygen demand (COD) and the absorbance measurements. The batch experiment results showed that the optimum conditions were: H_2O_2 dosage, 10,000 mg/L; Fe^{2+}dosage, 2,000 mg/L; initial concentration of organics, 413 mg/L; pH, 3 and temperature, 35 °C, under which the COD removal could reach 61.07% and fairly good stability could be obtained. Under the optimum experimental conditions, using UV irradiation to treat the wastewater, the photo-Fenton systems can successfully eliminate COD from guar gum solution. The COD removal always obeyed a pseudo-first-order kinetics and the degradation rate (k_{app}) was increased by 25.7% in the photo-Fenton process compared to the Fenton process. The photo-Fenton system needed less time and consequently less quantity of H_2O_2 to obtain the same results as the Fenton process. The photo-Fenton process needs a dose of H_2O_2 20.46% lower than that used in the Fenton process to remove 79.54% of COD. The cost of the photo/Fenton process amounted to RMB9.43/m^3, which was lower than that of the classic Fenton process alone (RMB10.58/m^3) and the overall water quality of the final effluent could meet the class I national wastewater discharge standard for the petrochemical industry of China.

Key words | degradation kinetics, economic analysis, Fenton, guar gum, oilfield wastewater, photo-Fenton

Shunwu Wang (corresponding author)
College of Chemistry and Chemical Engineering,
Northeast Petroleum University,
Daqing 163318,
China
E-mail: *15776575932@163.com*

Ziwang Li
College of Chemistry and Chemical Engineering,
Northeast Petroleum University,
Daqing 163318,
China

Qinglong Yu
Daqing Oilfield No. 4 Oil Production Plant Company Ltd,
Petrochina,
Daqing 163513,
China

INTRODUCTION

Large amounts of wastewater are generated during hydraulic fracturing to recover oil from deep shale formations (Aguilera 1995; Neghaban *et al.* 1998; Hickenbottom *et al.* 2013). This oilfield wastewater contains various organics pollutants, solid impurities, heavy metals, polymers, chemical additives, proppants, oil, etc. (Olsson *et al.* 2013). The wastewater is characterized by high chemical oxygen demand (COD), high color and salinity, strong acidity and viscosity, and has become one of the main sources of water pollution in oilfields and can increase considerably environmental hazards if discharged without effective treatment (Chase *et al.* 1997). Nowadays, disposal of wastewater constitutes one of the most significant waste discharges associated with oil well drilling (Yang *et al.* 2014), and consequently it is vital to explore appropriate processes for the effective abatement of organics to an acceptable level.

Among the several processes used in the treatment of these wastes, the advanced oxidation processes (AOPs) appear to be a promising field of study due to the effective degradation of organic contaminants under mild conditions (Andreozzi *et al.* 2000; Bautista *et al.* 2007). AOPs are based on the use of a very strong oxidizing agent such as hydroxyl radical ($HO^{\bullet}$) with oxidation-reduction potential ($HO^{\bullet}/H_2O$) = 2.8 V/NHE, which is generated *in situ* in the reaction medium (Hirvonen *et al.* 1996).

Fenton and UV-Fenton processes have proved to be effective and economical methods used for the detoxification and degradation of many organic compounds (Fusheng 1997; Yoon *et al.* 2001; Bagal & Gogate 2014). Oxidation with Fenton reagent is based on ferrous ion and hydrogen peroxide, and exploits the reactivity of the hydroxyl radical produced in acidic solution by the catalytic

doi: 10.2166/wst.2016.470

decomposition of H_2O_2 (Kang & Hwang 2000; Chamarro *et al.* 2001):

$$H_2O_2 + Fe^{2+} \rightarrow Fe^{3+} + OH^- + {}^{\bullet}OH \quad (1)$$

Ferrous iron is slowly regenerated through the so-called Fenton-like reaction between ferric iron and H_2O_2 in acidic aqueous medium (Sedlak & Andren 1991; Pan *et al.* 2008):

$$Fe^{3+} + H_2O_2 \rightarrow Fe^{2+} + HO_2^{\bullet} + H^+ \quad (2)$$

$$Fe^{3+} + HO_2^{\bullet} \rightarrow Fe^{2+} + O_2 + H^+ \quad (3)$$

Nevertheless, numerous competitive reactions can also occur, namely the following ones, which negatively affect the oxidation process (Bergendahl & Thies 2004; Ren 2014):

$$H_2O_2 + {}^{\bullet}OH \rightarrow HO_2^{\bullet} + H_2O \quad (4)$$

$${}^{\bullet}OH + Fe^{2+} \rightarrow Fe^{3+} + OH^- \quad (5)$$

$$H_2O_2 + HO_2^{\bullet} \rightarrow O_2 + HO^{\bullet} + OH^- \quad (6)$$

$$Fe^{2+} + HO_2^{\bullet} \rightarrow Fe^{3+} + HO_2^- \quad (7)$$

$$HO^{\bullet} + {}^{\bullet}OH \rightarrow H_2O_2 \quad (8)$$

$$HO^{\bullet} + HO_2^{\bullet} \rightarrow O_2 + H_2O \quad (9)$$

$$HO_2^{\bullet} + HO_2^{\bullet} \rightarrow O_2 + H_2O_2 \quad (10)$$

In the presence of substrate, as a target contaminant, the generated hydroxyl radicals are able to attack most of the contaminant either by hydrogen abstraction, as shown in Equation (11), or by hydroxyl addition, as shown in Equation (12) (Flotron *et al.* 2005; Sun *et al.* 2007), where R represents a saturated hydrocarbon group.

$$RH + {}^{\bullet}OH \rightarrow R^{\bullet} + H_2O \rightarrow \text{Products} \quad (11)$$

$$R + {}^{\bullet}OH \rightarrow OHR{\bullet} \rightarrow \text{Products} \quad (12)$$

In UV-Fenton process, in addition to the above reactions the formation of hydroxyl radical also occurs by the following reactions (Equations (13) and (14)).

$$Fe^{3+} + H_2O + hv \rightarrow Fe^{2+} + HO^{\bullet} + H^+ \quad (13)$$

$$H_2O_2 + hv \rightarrow 2{\bullet}OH \quad (14)$$

At acidic pH (2.5–5), the main compounds absorbing light in the UV-Fenton system are ferric ion complexes, e.g., $Fe(OH)^{2+}$ and $Fe(RCO_2)^{2+}$, which produce additional Fe^{2+}(Equations (15) and (16)) (Sagawe *et al.* 2001).

$$Fe(OH)^{2+} + hv \rightarrow Fe^{2+} + HO^{\bullet} \quad (15)$$

$$Fe(RCO_2)^{2+} + hv \rightarrow Fe^{2+} + R^{\bullet} + CO_2 \quad (16)$$

The rate of organic degradation could be increased by irradiation of Fenton with UV light. This leads not only to the formation of additional hydroxyl radicals but also to recycling of ferrous catalyst by reduction of Fe^{3+}. In this way, the concentration of Fe^{2+} is increased and the overall reaction is accelerated and can be used as alternative to UV lamps to reduce the degradation process costs. Thus, UV-Fenton degradation of contaminants using UV lamps has been successfully used as an economically viable process (Primo *et al.* 2008; Monteagudo *et al.* 2009).

The aim of this work is the optimization of the Fenton process for the degradation of guar gum as a main ingredient in oilfield wastewater. In order to improve the reaction rate, solutions were subjected to UV radiation using a laboratory-scale reactor. The influence of different operational parameters such as H_2O_2 dose, initial concentrations of organics and Fe^{2+}, temperature, and pH was investigated. Furthermore, the cost of the oilfield wastewater treatment in determining optimum Fenton reagent doses was also evaluated.

MATERIALS AND METHODS

Laboratory instruments and chemicals

An ultraviolet spectrophotometer (UV-8000, Metash Instrument Co., Ltd, China) and quartz cuvettes were used for measurements on absorbance analysis and COD using a dichromate solution as the oxidant in strong acid media. The pH values were determined by using an acidometer (PHS-3C, INESA Scientific Instrument Co., Ltd, China). Oxidation experiments were conducted with a six-joint heat-collection temperature magnetic stirrer (HJ-6, Changzhou ZOJE Experimental Instruction Manufacturing Co., Ltd, China). Ultraviolet radiation was generated through a

UV lamp (300 W, Metash Instrument Co., Ltd, China). A vacuum filtration device (FS3310, Shanghai Collar Germany Instrument Co., Ltd, China) is also needed for treating the effluent.

The hydrogen peroxide (H_2O_2, 30%, w/w), sodium hydroxide (NaOH), hydrochloric acid (HCl), ferrous sulfate heptahydrate ($FeSO_4{\cdot}7H_2O$), potassium dichromate ($K_2Cr_2O_7$) were of analytical grade, and other chemicals used were analytical reagent grade. All solutions were prepared with distilled water.

Oilfield wastewater was obtained from the National Offshore Oil Corporation at Tianjin, China. This wastewater was skimmed before being used and determined. The wastewater was stored at 4 °C until required. The main characteristics of sample wastewater are listed in Table 1. As shown, the oilfield wastewater had high concentrations of COD, total dissolved solids and suspended solids (SS). Moreover, the oilfield wastewater had high color.

Experimental setup

The experiments which involved UV radiation were carried out in a batch cylindrical glass photoreactor of 500 mL with a medium-pressure 300 W Hg lamp immersed in a quartz sleeve placed in the middle of the reactor. It was surrounded by a water cooling jacket to maintain constant temperature. A broad radiation spectrum was emitted with wavelengths from 200 nm to 600 nm, including complete range of ultraviolet radiation. To determine the amount of radiation emitted by the UV lamp, actinometric experiments were performed. The photon flux entering the reactor was 8.8×10^{-5} Einstein/s estimated from hydrogen peroxide actinometry (Nicole *et al.* 1990). A magnetic stirrer was used to provide proper mixing (Primo *et al.* 2007).

Table 1 | Characteristics of the raw oilfield wastewater

Parameter	Unit	Value
pH	/	6.7
COD	mg/L	3,386
BOD_5	mg/L	631
BOD_5/COD	/	0.186
Total dissolved solids	mg/L	6,150
SS	mg/L	40.38
Color	0	175
Guar gum	mg/L	3,297–3,516
Alkalinity	mg/L	5,126
Oil and grease	mg/L	37
Total petroleum hydrocarbon	mg/L	34

Experimental procedure

Prior to the experiments, to minimize particulate effects in oxidation reactions and to determine the organic matter corresponding to the solid fraction, the wastewater samples were filtered through a 0.45 μm millipore filter. After filtration, the initial COD concentration scarcely decreased 2–3% (Sedlak & Andren 1991). Batch experiments were carried out adjusting initial pH to 3–3.5 with sulfuric acid to enhance the oxidation. Then, hydrogen peroxide and ferrous sulfate heptahydrate were added to 200 mL wastewater samples using a six-joint heat-collection temperature magnetic stirrer to provide proper mixing and various temperature according to the treatment conditions. For tests using only the Fenton reagent, the experimental device was kept away from UV irradiation by covering with a black plastic film and an aluminum foil. After the oxidation reaction, neutralization was carried out by increasing pH value up to 8–9 with sodium hydroxide. After settling for 30 minutes, the samples was filtered by 0.45 μm membrane through the vacuum filtration device. Then, the absorbance and COD in the supernatant were measured.

All samples were tested in duplicate, and the test was reproduced three times for each sample, so that the relative errors could be minimized. All the figures show the average values.

RESULTS AND DISCUSSION

Oxidation of wastewater by the Fenton process

Kinetics of COD removal

Figure 1 shows the decrease of COD during the oxidation of guar gum ($COD_0 = 3{,}386$ mg/L) by Fenton's reagent. It can be seen that COD values decreased almost exponentially and 59% of COD removal was obtained after approximately 110 min. If we suppose that the oxidation of guar gum and its by-products by the hydroxyl radicals is of a first order with respect to COD and that the hydroxyl radicals concentration is constant during the treatment, the oxidation rate (r) can be given by the following equation:

$$r = \frac{dCOD}{dt} = k[HO^{\bullet}]^{\alpha} COD = k_{app} COD \quad (17)$$

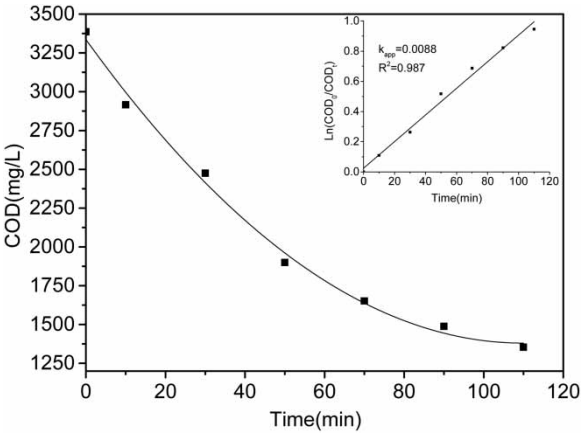

Figure 1 | Trend of COD during the oxidation of guar gum solution by Fenton process. The inset panel shows its kinetic analysis assuming that COD follows a pseudo-first-order reaction. Dosing of H_2O_2 10,000 mg/L, $[Fe^{2+}] = 2{,}000$ mg/L, pH = 3, and T = 35 °C.

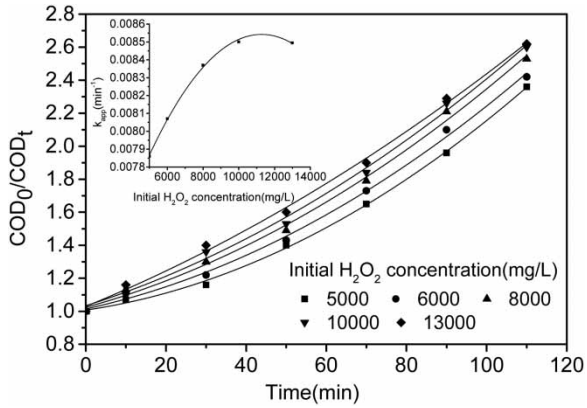

Figure 2 | Effect of H_2O_2 concentrations on the COD removal by the Fenton process. The inset panel shows k_{app} evolution at different dosing of H_2O_2. $COD_0 = 3{,}386$ mg/L, $[Fe^{2+}] = 2{,}000$ mg/L, pH = 3, and T = 35 °C.

where k is the reaction rate constant, α is the reaction order related to the hydroxyl radicals, and $k_{app} = k[\bullet OH]^{\alpha}$ the apparent rate constant. The integration of Equation (17) subject to the initial condition $COD = COD_0$ at $t = 0$ leads to the following equation:

$$COD_t = COD_0 \exp(-k_{app} t) \quad (18)$$

The value of k_{app} could be calculated from the plot of $Ln(COD_0/COD_t)$ versus t (inset of Figure 1). As can be seen, points lie satisfactory in a straight line with correlation coefficient greater than 0.96. The constant k_{app} was used to study the effect of different concentrations of H_2O_2, Fe^{2+} and guar gum, and different temperatures and pH.

Effect of H_2O_2 concentrations

The H_2O_2 dose is considered as one of the most important factors which should be considered in the Fenton process (Bagal & Gogate 2014). The effect of the dosing of hydrogen peroxide on the efficiency of the oxidation process was investigated under the operating conditions ($COD_0 =$ 3,386 mg/L, $[Fe^{2+}] = 2{,}000$ mg/L, pH = 3, and T = 25 °C (Figure 2). It was found that COD removal efficiency increases with increasing the concentrations of hydrogen peroxide from 5,000 to 13,000 mg/L. The highest percent removal of COD was attained at 110 min when using 10,000 mg/L H_2O_2 concentration, so further addition of H_2O_2 is not necessary. Excessive H_2O_2 reacts with $HO^{\bullet}$ competing with organic pollutants and consequently reduces treatment efficiency (Pinar *et al.* 2013; Pliego *et al.* 2014).

The inset of Figure 2 shows the variation of the apparent rate constant (k_{app}) values, at different H_2O_2 concentrations, calculated from the straight lines considering a pseudo-first-order reaction. The value of k_{app} increased when the concentration of H_2O_2 increased from 5,000 to 10,000 mg/L, then began to decline from 10,000 to 13,000 mg/L. This is due to the effect of the additional $HO^{\bullet}$ radicals produced. Given that the concentration of Fe^{2+} introduced initially in the solution is sufficient to react with H_2O_2, the competitive reactions (Equations (4), (6), and (8)–(10)) did not affect significantly the COD removal rate.

Furthermore, in order to follow the change in solution color during guar gum oxidation, absorbance measurements were carried out at a wavelength of 254 nm. In the first 10 minutes, the solution undergoes a fast color change from yellow to dark brown, reaching a peak level. Later, the solution begins to slowly clear to a light brown, and even turns a pale yellow residual color in some experimental conditions. The effect of concentration of hydrogen peroxide on color evolution was tested in a set of assays with constant catalyst concentration $[Fe^{2+}] = 2{,}000$ mg/L at pH 3. Results are reported in Figure 3, which shows the temporal absorbance at 254 nm using different concentration of H_2O_2. In all cases, the COD removal efficiency is lower than color removal efficiency during guar gum oxidation. The rate of this decolorization stage increased with the increase of concentration of H_2O_2 and the solution being fully decolorized at shorter reaction times. With 10,000 mg/L H_2O_2 dose, the initial absorbance has a maximum ($A_{254} = 0.517$) after about 110 min of treatment and then the absorbance decreased and tended to 0.05, leading to the almost complete disappearance of color. The relationship between the dose of hydrogen peroxide and the final color of the solution is

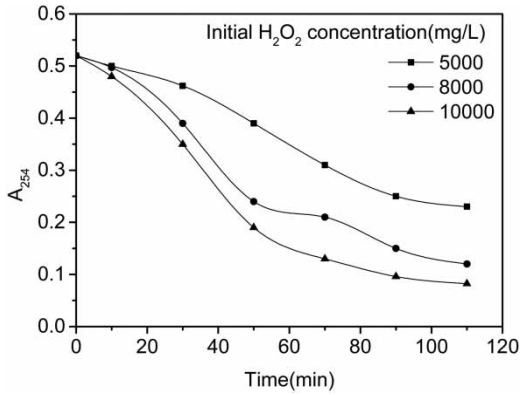

Figure 3 | Temporal results of color evolution at 254 nm (A_{254}). Effect of the concentration of H_2O_2 upon color formation and abatement. $COD_0 = 3{,}386$ mg/L, $[Fe^{2+}] = 2{,}000$ mg/L, pH = 3, and T = 35 °C.

therefore established, and it is concluded that the color observed depends on the level of oxidation reached. Consequently, it can be said that current color is a good indicator of the degree of oxidation achieved during the reaction. Using at least 10,000 mg/L H_2O_2 dose is required in these conditions to remove almost completely the guar gum.

Effect of the initial concentration of ferrous iron

Ferrous ion acts as a catalyst in Fenton's reactions (Wang *et al.* 2014; Oh *et al.* 2016). To choose the optimal amount of Fe^{2+} added in the reaction solution, a set of tests was performed. Figure 4 illustrates the decrease of COD with time, during the oxidation of guar gum wastewater ($COD_0 =$ 3,386 mg/L) using different initial concentrations of Fe^{2+}. As can be seen, Fe^{2+} dosage has a significant effect on the degradation of guar gum. The COD percent removal increased from 48% to 55.2% within 110 min reaction when the initial concentration of Fe^{2+} increased from 1,000 to 2,000 mg/L. As a catalyst, ferrous ion initiates the decomposition of hydrogen peroxide to generate the very reactive $HO^{\bullet}$ in Fenton's reactions. Therefore, higher initial Fe^{2+} concentration led to higher generation of $HO^{\bullet}$ and better degradation of guar gum solution and its by-products. However, for Fe^{2+} doses higher than 2,000 mg/L, the COD percent removal showed almost no change. This result is essentially due to competitive consumption of $HO^{\bullet}$ and $HO_2^{\bullet}$ radicals (Equations (5) and (7)) (Buxton *et al.* 1988). It is worth noting that, in the Fenton process, the amounts of Fe^{2+} ions should be as low as possible for economic and environmental reasons; high amounts of Fe^{2+} ions might produce a larger quantity of Fe^{3+} sludge. The treatment of the sludge containing Fe^{3+} at the end of the wastewater treatment is expensive and needs a large amount of chemicals and manpower.) (Ramirez *et al.* 2007; Hansson *et al.* 2015).

On the other hand, the inset of Figure 4 shows that k_{app} values, calculated from the straight lines, considering a pseudo-first-order reaction, increased as a function of Fe^{2+} dosage and reached a maximum around 2,000 mg/L of Fe^{2+}. Therefore, 2,000 mg/L Fe^{2+} was selected as the optimum Fe^{2+} dosage in this work.

Moreover, Figure 5 shows the change in absorbance of the solution versus time measured for four initial concentrations of Fe^{2+} ions. In all cases the curves showed the same shape. The absorbance decreased from an initial maximum whose intensity increased proportionally with the amount of Fe^{2+} ions. The final color can be deepened or modified by Fe^{3+} that appears in the reacting medium due to the oxidation of Fenton reagent. Colored chemical additive compounds are the main contributors to the color

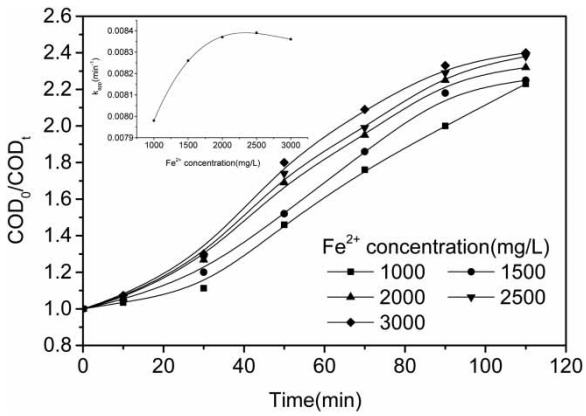

Figure 4 | Effect of the initial concentration of Fe^{2+} on the COD removal by Fenton process. The inset panel shows k_{app} evolution at different Fe^{2+} concentration. $COD_0 = 3{,}386$ mg/L, concentration of H_2O_2 10,000 mg/L, pH = 3, and T = 35 °C.

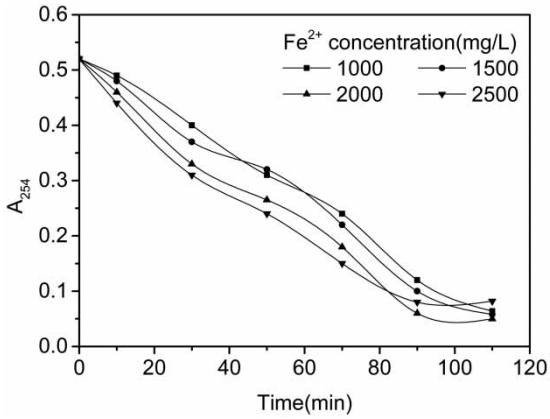

Figure 5 | Temporal results of color evolution at 254 nm (A_{254}). Effect of the initial concentration of ferrous ions upon color formation and abatement. $COD_0 =$ 3,386 mg/L, concentration of H_2O_2 10,000 mg/L, pH = 3, and T = 35 °C.

observed during the reaction, although the contribution of Fe^{3+} and its complexes is by no means negligible because the residual color of fully oxidized water increases with the initial concentration of iron. This suggestion is also supported by other authors (Federico *et al.* 2006).

Effect of the initial COD

It is important from an application point of view to study the dependence of removal efficiency on the initial concentration of the organics pollutant. Therefore, the effect of guar gum concentration on the degradation efficiency was investigated at different initial concentrations (COD_0, 413, 792, 1,690, and 3,386 mg/L) and results are presented in Figure 6. It can be observed that the COD removal decreased with the increase of the initial concentration of the pollutant. Almost 80%, 75%, 68% and 59% of COD removal was achieved after about 110 min time of reaction for COD_0 413, 792, 1,690, and 3,386 mg/L, respectively. However, at high concentration, the removal of COD needs more time and so more H_2O_2; this is because when the concentration of COD increases, the quantity of hydroxyl radicals produced continuously with time does not increase accordingly and hence the removal rate decreases. Also, from the inset of Figure 6, it can be seen that k_{app} decreased linearly with COD_0. This behavior was similar to those reported by many researchers (Modirshahla *et al.* 2007; Francisco 2016).

Effect of the initial pH

The effects of pH on the degradation of guar gum organics by the Fenton reaction has been illustrated and acidic conditions are required to produce the maximum amount of HO• by the decomposition of H_2O_2 catalyzed by ferrous ions (Xie *et al.* 2015). Several investigations have indicated that the optimum pH for the degradation of organics by the Fenton process is in the range 2.5–3.5 and that the extent of degradation decreases with increasing pH for pH > 3.5 (Samet *et al.* 2009).

Figure 7 shows the change of COD removal with time and the k_{app} curve in the oxidation of guar gum solution ($COD_0 = 3{,}386$ mg/L) as a function of the initial pH. Compared with 59.6% at pH 2 and 57.6% at pH 4, the optimum pH point of COD removal is 3 with 62.8%. Obviously, the COD removal efficiency was influenced by the initial pH and the optimum experiment pH was 3. The values of k_{app} increase when pH increases from 2 to 3, then decrease when pH is raised from 3 to 6. The contributing factors for the low k_{app} in lower pH range (<3) include the formation of oxonium ion (i.e., $H_3O_2^+$) due to the strong proton solvating ability of H_2O_2, complex species $[Fe(H_2O)_6]^{2+}$ and $[Fe(H_2O)_6]^{3+}$ and enhanced HO• scavenging by H^+. The poor degradation of guar gum at a high pH value (>3) was caused by the formation of ferrous and ferric hydroxide complexes with much lower catalytic capability than Fe^{2+} (Kang & Wang 2000; Zhao & Hu 2008).

In addition, the influence of the initial pH on the evolution with time of the absorbance at 254 nm wavelength is shown in Figure 8. As can be seen, initial pH has no significant effect on the final color removal efficiency at pH values between 2 and 5 and can lead to the almost disappearance of color at the end of the treatment.

Effect of the temperature

The temperature plays an important role in chemical oxidation, because it represents a determinant parameter in

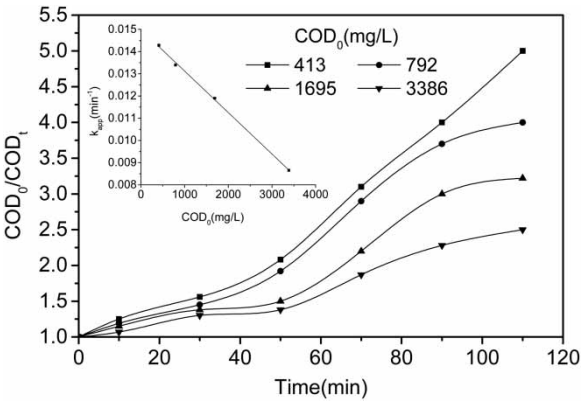

Figure 6 | Effect of the initial concentration of guar gum on the COD removal by the Fenton process. The inset panel shows k_{app} evolution at different initial COD. Concentration of H_2O_2 10,000 mg/L, $[Fe^{2+}] = 2{,}000$ mg/L, pH = 3, and T = 35 °C.

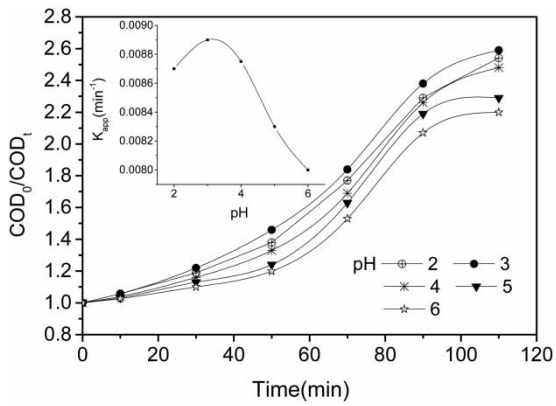

Figure 7 | Effect of the initial pH on the COD removal by the Fenton process. The inset panel shows k_{app} evolution at different pH. Concentration of H_2O_2 10,000 mg/L, $[Fe^{2+}] = 2{,}000$ mg/L and T = 35 °C.

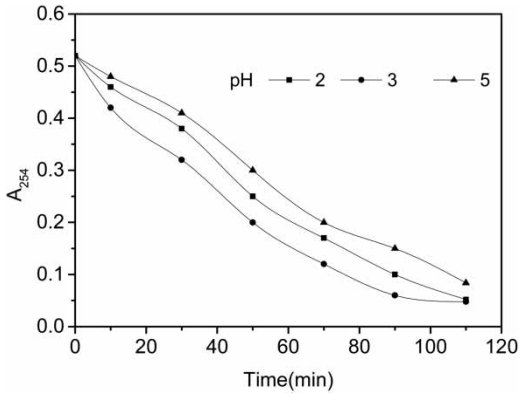

Figure 8 | Temporal results of color evolution at 254 nm (A_{254}). Effect of the initial pH upon color formation and abatement. Concentration of H_2O_2 10,000 mg/L, $[Fe^{2+}] = 2{,}000$ mg/L and T = 35 °C.

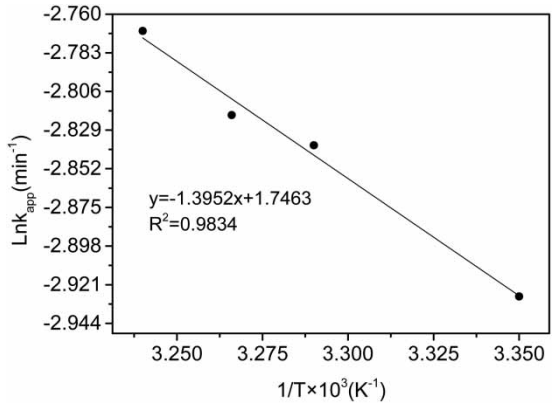

Figure 10 | Plot of Ln k_{app} versus (1/T) for the degradation of guar gum by Fenton oxidation process. $COD_0 = 3{,}386$ mg/L, concentration of H_2O_2 10,000 mg/L, $[Fe^{2+}] = 2{,}000$ mg/L and pH = 3.

the kinetics of homogeneous reactions. The influence of this parameter on the kinetic rate constant, k_{app}, for the guar gum degradation was investigated in the range between 25 °C and 60 °C with test conditions at COD_0 3,386 mg/L, H_2O_2 10,000 mg/L, Fe^{2+} 2,000 mg/L and pH 3. The obtained results shown in Figure 9 indicate that k_{app} was significantly influenced by the temperature with an optimal value of 35 °C. The values of k_{app} quickly increased when the temperature increased from 25 °C to 35 °C, suddenly decreased when the temperature was raised from 35 °C to 50 °C, and then gradually decreased with the increase of temperature in the range of 50–60 °C. The decrease of k_{app} at temperature higher than 35 °C is due to the accelerated decomposition of H_2O_2 into oxygen and water. Similar results were reported by researchers (Wang 2008). The data for temperatures between 25 °C and 35 °C exhibit an Arrhenius-type behavior with apparent activation energy of 17,543 J/mol (Equation (19)) calculated from the usual Lnk$_{app}$ versus 1/T (Figure 10).

$$k_{app} = 58.78 \exp\left(\frac{-17,543}{RT}\right) min^{-1} \quad (19)$$

where R is the ideal gas constant (8.314 J/mol K) and T is the reaction absolute temperature (K).

Oxidation of wastewater by the UV-Fenton process

In order to improve the reaction rate and COD abatement efficiency, solutions were subjected to UV radiation using a laboratory-scale reactor. Figure 11 shows the trend of the COD_0/COD_t ratio during the treatment of wastewater by the two processes under the optimum experimental conditions already found when using the Fenton process

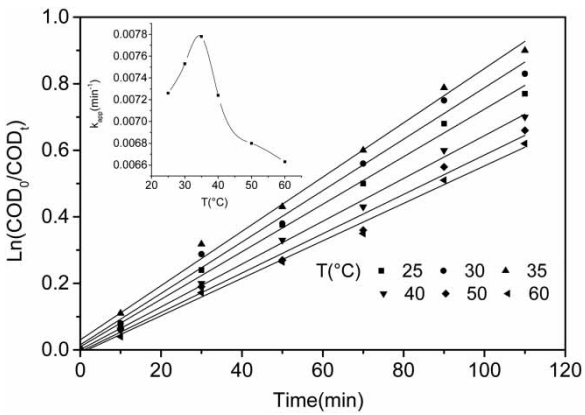

Figure 9 | Plot of Ln(COD_0/COD) versus time at different temperatures. $COD_0 = 3{,}386$ mg/L, concentration of H_2O_2 10,000 mg/L, $[Fe^{2+}] = 2{,}000$ mg/L and pH = 3.

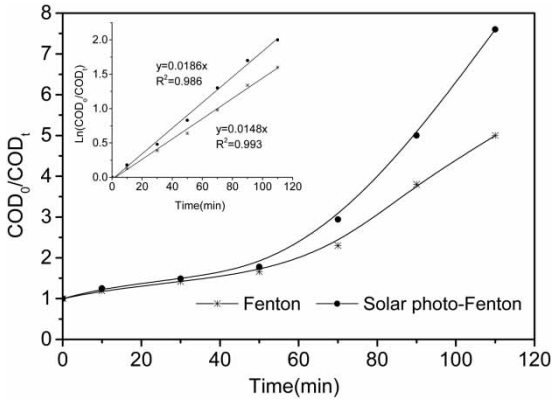

Figure 11 | Effect of UV radiation on the kinetic abatement of COD during the treatment of wastewater ($COD_0 = 413$ mg/L). The inset panel shows the fitting of the experimental data to a first-order reaction kinetic model concentration of H_2O_2 10,000 mg/L, $[Fe^{2+}]$ 2,000 mg/L, pH = 3 and T 35 °C.

Table 2 | Consumption of the reagents and their costs

	Dosage (kg/m^3)					
Treatment technology	**HCl**	**NaOH**	**$FeSO_4{\cdot}7H_2O$**	**H_2O_2**	**UV (W)**	**Operating cost (RMB/m^3)**
Fenton process	0.015	0.05	2	10	0	10.58
Photo/Fenton process	0.015	0.05	1.793	7.986	300	9.43

Note: Unit price of reagent (RMB/t): HCl, 100; NaOH, 2,000; $FeSO_4{\cdot}7H_2O$ (99.0 wt.% purity), 240; H_2O_2 (30%, w/w), 1,000; UV lamp (300 W), 0.5 RMB (KW/h).

(COD_0 413 mg/L, concentration of H_2O_2 10,000 mg/L, [Fe^{2+}] 2,000 mg/L, pH = 3 and T 35 °C). It can be seen that the UV-Fenton system needed less time to reach the same COD removal efficiency. After reaction, the concentration of residual H_2O_2 in solution is 2,046 mg/L, and consequently a smaller quantity of H_2O_2 is required to reach the maximum COD removal. In fact, under the optimum experimental conditions, the UV-Fenton process need a dose of H_2O_2 20.46% lower than that used in the Fenton process to remove 79.54% of COD. Furthermore, the COD removal rate is higher with the UV-Fenton process as shown by the k_{app} values in the inset of Figure 11.

Economic analysis

An efficient and cost-effective treatment process must strike a balance between treatment efficiency and operating costs. The consumption of the chemical reagents in the treatment technology of photo/Fenton and classic Fenton alone are shown in Table 2. The cost of the treatment of the classic Fenton process alone was about RMB10.58/m^3, while in the case of the photo/Fenton process, the cost was only RMB9.43/m^3 when met with the same COD discharge requirement. From the perspective of economy, the photocatalytic process reduced the cost of H_2O_2 in the subsequent Fenton process, thereby resulting in lower treatment cost. This indicated that the photo/Fenton process was more economical for the degradation of oilfield wastewater. Thus the photo/Fenton process can be potentially used in industrial applications.

CONCLUSION

On the basis of the experimental data obtained in this study, the degradation of guar gum has been studied by applying homogeneous Fenton and photo-Fenton processes. The results showed that the photo-Fenton process was more efficient than the Fenton process for COD removal. In the photo-Fenton process, the degradation rate (k_{app}) was increased by 25.7%, which reduced the operating cost greatly. Furthermore, the COD and color removal increased with the increase of the concentration of hydrogen peroxide, the ferrous ion as catalyst accelerated the COD removal, and Fe^{2+} concentration of 2,000 mg/L could be used as an optimum dosage for the Fenton process. Furthermore, the optimum pH for both COD and color removal was 3. In addition, the degradation rate was significantly influenced by the temperature with an optimum value of 35 °C.

The costs of the photo/Fenton process amounted to RMB9.43/m^3. Therefore, the photo-Fenton process can be considered as an effective, alternative and economic method for the treatment of oilfield wastewater.

ACKNOWLEDGEMENTS

The authors thank the kind help of China National Offshore Oil Corporation in Tianjin for providing water samples.

REFERENCES

Aguilera, R. 1995 *Naturally Fractured Reservoirs*, 2nd edn. PennWell Publishing, Tulsa, Oklahoma, USA.

Andreozzi, R., Caprio, V., Insola, A., Marotta, R. & Sanchirico, R. 2000 Advanced oxidation processes for the treatment of mineral oil-contaminated wastewaters. *Water Res.* **34**, 620–628.

Aytar, P., Gedikli, S., Sam, M., Farizoğlu, B. & Çabuk, A. 2013 Sequential treatment of olive oil mill wastewater with adsorption and biological and photo-Fenton oxidation. *Environ. Sci. Pollut. Res.* **20** (5), 3060–3067.

Bagal, M. V. & Gogate, P. R. 2014 Wastewater treatment using hybrid treatment schemes based on cavitation and Fenton. Chemistry: a review. *Ultrason. Sonochem.* **21**, 1–14.

Bautista, P., Mohedano, A. F., Gilarranz, M. A., Casas, J. A. & Rodriguez, J. J. 2007 Application of Fenton oxidation to cosmetic wastewaters treatment. *Journal of Hazardous Materials* **143** (1–2), 128–134.

Bergendahl, J. A. & Thies, T. P. 2004 Fenton's oxidation of MTBE with zerovalent iron. *Water Res.* **38**, 327–334.

Buxton, G. V., Grennstock, C. L., Helman, W. P. & Ross, A. B. 1988 Critical review of rate constants for reactions of

hydrated electrons, hydrogen atoms and hydroxyl radicals OH·/O·⁻ in aqueous solution. *J. Phys. Chem.* **17**, 513–886.

Chamarro, E., Marco, A. & Esplugas, S. 2001 Use of Fenton reagent to improve organic chemical biodegradability. *Water Res.* **35**, 1047–1051.

Chase, B., Chmicowski, W., Marcinewr, R., Mitchell, C., Dang, Y., Krauss, K., Nelson, E., Lantz, T., Parham, C. & Plummer, J. 1997 Clear fracturing fluids for increased well productivity. *Oilfield Review* **9** (3), 20–23.

Federico, M., Fernando, V. & Natalia, V. 2006 Changes in solution color during phenol oxidation by Fenton reagent. *Environ. Sci. Technol.* **40**, 5538–5543.

Flotron, V., Delteil, C. & Padellec, Y. 2005 Removal of sorbed polycyclic aromatic hydrocarbons from soil, sludge and sediment samples using the Fenton's reagent process. *Chemosphere* **59**, 1427–1437.

Francisco, E. 2016 Effect of photo-Fenton reaction on physicochemical parameters in white wine and its influence on ochratoxin A contents using response surface methodology. *Eur. Food Res. Technol.* **242** (1), 91–106.

Fusheng, W. 1997 *Guide to Water and Wastewater Monitoring Analysis Method* Vol. 2. Chinese Environment Science Press, Beijing (in Chinese).

Hansson, H., Kaczala, F., Marques, M. & Hogland, W. 2015 Photo-Fenton and Fenton oxidation of recalcitrant wastewater from the wooden floor industry. *Water Envir. Res.* **87** (6), 491–497.

Hickenbottom, K. L., Hancock, N. T., Hutchings, N. R., Appleton, E. W., Beaudry, E. G., Xua, P. & Cath, T. Y. 2013 Forward osmosis treatment of drilling mud and fracturing wastewater from oil and gas operations. *Desalination* **312**, 60–66.

Hirvonen, A., Tuhkanen, T. & Kalliokoski, P. 1996 Formation of chlorinated acetic acids during UV/H_2O_2 oxidation of ground water contaminated with chlorinated ethylene. *Water Sci. Technol.* **32**, 1091–1102.

Kang, Y. W. & Hwang, K. Y. 2000 Effects of reaction conditions on the oxidation efficiency in the Fenton process. *Water Res.* **34**, 2786–2790.

Modirshahla, N., Behnajady, M. A. & Ghanbary, F. 2007 Decolorization and mineralization of C.I. acid yellow 23 by Fenton and photo-Fenton processes. *Dyes Pigm.* **73**, 305–310.

Monteagudo, J. M., Durán, A. & San Martín, I. 2009 Effect of continuous addition of H_2O_2 and air injection on ferrioxalate assisted solar photo-Fenton degradation of Orange II. *Appl. Catal. B Environ.* **89**, 510–518.

Neghaban, S., May, E., Britt, K. & Nolte, K. 1998 *The Effect of Yield Stress on Fracture Fluid Cleanup Inclusion of Gravity Effects*. SPE, New Orleans, USA.

Nicole, I., De Laat, J., Dore, M., Duguet, J. P. & Bonnel, C. 1990 Use of UV radiation in water treatment: measurement of photonic flux by hydrogen peroxide actinometry. *Water Res.* **24**, 157–168.

Olsson, O., Weichgrebe, D. & Rosenwinkel, K. H. 2013 Hydraulic fracturing wastewater in Germany: composition, treatment, concerns. *Environ. Earth Sci.* **1**, 1–12.

Oh, H. S., Kim, J.-J. & Kim, Y. H. 2016 Stabilization of hydrogen peroxide using tartaric acids in Fenton and Fenton-like oxidation. *Korean Journal of Chemical Engineering* **33** (3), 885–892.

Pan, Y. X., Zheng, H. L., Li, D. D. & Gou, Q. 2008 Degradation of organics in landfill leachate by ultrasound/Fenton process. *Chin. J. Environ. Eng.* **2** (4), 445–449.

Pliego, G., Zazo, J. A., Pariente, M. I., Rodríguez, I., Petre, A. L., Leton, P. & García, J. 2014 Treatment of a wastewater from a pesticide manufacture by combined coagulation and Fenton oxidation. *Environmental Science and Pollution Research* **21** (21), 12129–12134.

Primo, O., Rivero, M. J., Ortiz, I. & Irabien, A. 2007 Mathematical modelling of phenol photooxidation: kinetics of the process toxicity. *Chem. Eng. J.* **134**, 23–28.

Primo, O., Rivero, M. J. & Ortiz, I. 2008 Photo-Fenton process as an efficient alternative to the treatment of landfill leachates. *Journal of Hazardous Materials* **153**, 834–842.

Ramirez, J. H., Costa, C. A., Madeira, L. M., Mata, G., Vicente, M. A, Rojas-Cervantes, M. L, López-Peinado, A. J. & Martín-Aranda, R. M. 2007 Fenton-like oxidation of orange II solutions using heterogeneous catalysts based on saponite clay. *Appl. Catal. B Environ.* **71**, 44–56.

Ren, L. 2014 *Study on Pretreatment of a Pharmaceutical Wastewater by Tron-carbon Micro-electrolysis & Fenton Reagent*. Environmental Engineering of Chongqing University (in China).

Sagawe, G., Lehnard, A. & Lubber, M. 2001 The insulated solar Fenton hybrid process: fundamental investigations. *Helv. Chim. Acta* **84**, 3742–3759.

Samet, Y., Ayadi, M. & Abdelhédi, R. 2009 Degradation of 4-chloroguaiacol by dark Fenton and solar photo-Fenton advanced oxidation processes. *Water Environ. Res.* **8**, 2389–2397.

Sedlak, D. L. & Andren, A. W. 1991 Oxidation of chlorobenzene with Fenton's reagent. *Environ. Sci. Technol.* **25** (4), 777.

Sun, J. H., Sun, S. P., Fan, M. H. & Guo, H. Q. 2007 A kinetic study on the degradation of p-nitroaniline by Fenton oxidation process. *J. Hazard. Mater.* **148**, 172–177.

Wang, S. 2008 A comparative study of Fenton and Fenton-like reaction kinetics in decolorisation of wastewater. *Dyes Pigm.* **76**, 714–720.

Wang, C., Zhang, S., Yuji, S. & Zhang, Z. 2014 Analysis of a complex produced in the Fenton oxidation process. *Water Sci. Technol.* **69** (5), 1115–1119.

Xie, G., Zhou, L., Gao, W. & Li, Y. 2015 Organic additives enhance Fenton treatment of nitrobenzene at near-neutral pH. *Environ. Sci. Pollut. Res.* **22** (9), 7082–7092.

Yoon, J., Lee, Y. & Kim, S. 2001 Investigation of the reaction pathway of ·OH radicals produced by Fenton oxidation in the conditions of wastewater treatment. *Water Sci. Technol.* **44** (5), 15–21.

Yang, J., Hong, L., Liu, Y.-H., Guo, J.-W. & Lin, L.-F. 2014 Treatment of oilfield fracturing wastewater by a sequential combination of flocculation, Fenton oxidation and SBR process. *Environ. Technol.* **35** (22), 2878–2884.

Zhao, Y. & Hu, J. 2008 Photo-Fenton degradation of 17β-estradiol in presence of α-FeOOHR and H_2O_2. *Appl. Catal. B Environ.* **78** (3–4), 250–258.

First received 6 June 2016; accepted in revised form 22 September 2016. Available online 7 October 2016